

ON THE MODELLING AND SIMULATION OF HIGH PRESSURE PROCESSES AND INACTIVATION OF ENZYMES IN FOOD ENGINEERING

J.A. Infante*, B. Ivorra†,
Á.M. Ramos‡ and J.M. Rey§

Departamento de Matemática Aplicada,
Universidad Complutense de Madrid
Plaza de Ciencias, 3, 28040–Madrid, Spain

*ja_infante@mat.ucm.es, †ivorra@mat.ucm.es, ‡angel@mat.ucm.es, §jose_rey@mat.ucm.es

28 Enero, 2009

Abstract

High Pressure (HP) Processing has turned out to be very effective in prolonging the shelf life of some food. This paper deals with the modelling and simulation of the effect of the combination of high pressure and thermal treatments on food processing, focussing on the inactivation of certain enzymes. The behaviour and stability of the proposed models are checked by various numerical examples. Furthermore, various simplified versions of these models are presented and compared with each other in terms of accuracy and computational time. The models developed in this paper provide a useful tool to design suitable industrial equipments and optimize the processes.

Keywords: Modelling; Sensitivity Analysis; Food Technology; High Pressure; Heat and Mass Transfer; Inactivation of Enzymes; Simulation.

AMS Subject Classification: 35Q30, 65N30, 76D05, 76N99, 80A20.

1 Introduction

At present, the demand of safe and minimally processed food prepared for immediate consumption (ready-to-use and ready-to-eat) has increased significantly, in order to meet the needs of restaurants, collective dining rooms (colleges, companies, hospitals, residences, etc.) as well as domestic consumption.

One of the technologies that can be used for the preparation of these products is High Pressure (HP) processing, which has turned out to be very effective in prolonging the shelf life of some foods (cooked ham, juices, guacamole, oysters, etc.), being already a reality at an industrial level. One of the great advantages of this process is that they do not use additives, which consumers prefer to elude. Also, it avoids the use of high temperatures during the process (not like Pasteurization), which may have adverse effect on some nutritional properties of the food, its flavor, etc. (see, e.g., [10] and [11]).

Nomenclature			
A	Enzymatic activity	T	Temperature
A_1, A_2	Corner points	T_0	Initial temperature
AEA	Average activity error	T_r	Refrigeration/heating temperature
AET	Average temperature error	T_{amb}	Ambient temperature
B_1, B_2	Points located on the sample	\mathbf{u}	Fluid velocity field
BSAA	Bacillus Subtilis α -Amylase	V	Volumen
C_p	Heat capacity	X	Trajectory of a food particle
CPE	Carrot Pectin Methyl-Esterase	z	Vertical coordinate
EA	Activity error	∇	Gradient
ET	Temperature error	$\nabla \cdot$	Divergence
\mathbf{g}	Gravity vector	∇^2	Laplacian
H	Domain height		
h	Heat transfer coefficient		
I	Identity tensor		
k	Thermal conductivity	α	Thermal expansion coefficient
L	Domain width	Γ	Whole domain boundary
LB	Simplified Boussinesq model	Γ_r	Known temperature boundary
LCC	Simplified model with constant coefficients for liquid type food	Γ_{up}	Heat transfer boundary
LFull	Full model for liquid type food	$\Delta\nu$	Compressibility factor
LOX	Lipoxygenase	$\Delta\zeta$	Thermal expansibility factor
M	Mass	η	Dynamic viscosity
$\mathcal{M}(f; D)$	Mean value of a function f in a domain D	κ	Inactivation rate
\mathbf{n}	Outward normal unit vector	ρ	Density
N	Amount of perturbed models	τ	Time step
P	Equipment pressure	Ω	Whole domain
p	Mass transfer pressure	Ω_C	Cap of the sample holder
r	Radial coordinate	Ω_F	Sample food domain
R	Universal gas constant	Ω_P	Pressurizing medium domain
RAET	Relative value for AET	Ω_S	Vessel wall domain
RET	Relative value for ET		
S	Entropy		
SCC	Simplified model with constant coefficients for solid type food	<i>Indices</i>	
SFull	Full model for solid type food	*	Rotated domains
t	Time	F	Food sample
t_f	Final time	P	Pressurizing fluid
		per	Perturbed model
		ref	Reference value
		sim	Simplify model

This paper deals with the modelling and simulation of the effect of the combination of high pressure and thermal treatments on food processing, focussing on the inactivation of certain enzymes. Other studies for this kind of problems can be seen, for instance, in [4, 8] and [9]. Due to the high computational complexity needed to solve the full models (which include heat and mass transfer and non-constant thermophysical properties), we are also going to consider and to study some simplified versions of them. All of these models might become very important in order to design suitable industrial equipments and optimize the processes.

In Section 2 some models for enzymatic inactivation are presented. These models need the pressure and temperature profiles as an input. These quantities are obtained by means of the full and the simplified models developed in Section 3, where we also propose a sensitivity analysis. In Section 4 we couple those models in order to get numerical results for the distribution of temperature and inactivation of enzymes. Finally, in Section 5 we outline the final remarks, describing the steps proposed to optimize a thermal-HP process for any particular food and equipment.

2 Mathematical model for enzymatic inactivation

In order to predict the impact that HP–thermal processes have on the activity of some enzymes in food, we have implemented a particular first order kinetic model. Basically, it describes the evolution of the activity which depends on the pressure and the temperature, which are needed as an input for the model.

Several experimental protocols may be used to measure the enzymatic activity: typically, they take into account the variation of a suitable magnitude (for instance, oxygen concentration [12], optical density [21], carboxylgroups released from a pectin [22]) per time unit. According to the chosen magnitude, this activity is expressed in the corresponding units ($(\Delta\text{ppm of O}_2) \text{ s}^{-1}$, $\text{cm}^{-1} \text{ min}^{-1}$, $(\text{mL of } 0.01M \text{ NaOH}) \text{ min}^{-1}$ for the magnitudes expressed above, respectively).

The evolution of the activity A of an enzyme is often described by the following first–order kinetic equation [24, 30]:

$$\frac{dA}{dt}(t) = -\kappa(P(t), T(t)) A(t), \quad (1)$$

where t is the time (min), $P(t)$ is the pressure (MPa) at time t , $T(t)$ is the temperature (K) at time t , $\kappa(P, T)$ is the inactivation rate (min^{-1}) corresponding to the pressure–temperature conditions given by (P, T) and $A(t)$ is the activity of the enzyme under study.

In the literature, several mathematical formulae that describe $\kappa(P, T)$ can be found. They are usually based on equations that model the pressure–temperature dependence of chemical reactions and they are chosen depending on the enzyme being studied.

Equation (1) provides a macro behaviour of the enzymatic activity. Nevertheless, it is not capable of capturing the non–homogeneous activity distribution that could appear (due to non–homogeneous temperature distribution) inside the food. Here we restrict the exposition to two equations that describe some types of enzymatic inactivation, which are then going to be used for numerical simulations in Section 4:

- The first equation is provided by a suitable combination of Arrhenius equation (modelling the temperature dependence) and Eyring equation (modelling the pressure dependence) [21]:

$$\kappa(P, T) = \kappa_{\text{ref}} \exp\left(-B\left(\frac{1}{T} - \frac{1}{T_{\text{ref}}}\right)\right) \exp(-C(P - P_{\text{ref}})), \quad (2)$$

where T_{ref} is a reference temperature (K), P_{ref} is a reference pressure (MPa), κ_{ref} is the inactivation rate at reference conditions (min^{-1}), B is the parameter that expresses the temperature dependence of κ (K) and C is the parameter that expresses the pressure dependence of κ (MPa^{-1}).

- The second equation is obtained by considering Eyring’s transition state theory adapted to enzymatic study [12, 22]:

$$\begin{aligned} \kappa(P, T) = & \kappa_{\text{ref}} \exp\left(\frac{-\Delta V_{\text{ref}}}{RT}(P - P_{\text{ref}})\right) \exp\left(\frac{\Delta S_{\text{ref}}}{RT}(T - T_{\text{ref}})\right) \\ & \exp\left(\frac{\Delta \nu}{2RT}(P - P_{\text{ref}})^2\right) \exp\left(\frac{-2\Delta \zeta}{RT}(P - P_{\text{ref}})(T - T_{\text{ref}})\right) \\ & \exp\left(\frac{\Delta C_p}{RT}\left(T\left(\ln\frac{T}{T_{\text{ref}}}\right) - 1\right) + T_{\text{ref}}\right) + \text{high order terms,} \end{aligned} \quad (3)$$

where $R = 8.314 \text{ (J mol}^{-1}\text{K}^{-1})$ is the universal gas constant, ΔV_{ref} is the volume change at reference conditions ($\text{cm}^3 \text{ mol}^{-1}$), ΔS_{ref} is the entropy change at reference conditions ($\text{J mol}^{-1}\text{K}^{-1}$), ΔC_p is the heat capacity change ($\text{J mol}^{-1}\text{K}^{-1}$), $\Delta \zeta$ is the thermal expansibility factor ($\text{cm}^3 \text{ mol}^{-1}\text{K}^{-1}$) and $\Delta \nu$ is the compressibility factor ($\text{cm}^6 \text{ J}^{-1} \text{ mol}^{-1}$). Depending on the enzyme that is being studied, higher order terms can be added to (3) in order to refine the approximation of the pressure–temperature dependence of the activity [22].

The parameters of the selected equation have been estimated using regression techniques on the data provided by experimental measurements of the activity [5]. We point out that they may depend on the enzymatic production lots used in the experiment (see, for instance, [21]).

Once the equation and parameters of κ have been obtained, the solution at time t of (1) is obviously given by

$$A(t) = A(0) \exp \left(- \int_0^t \kappa(P(\sigma), T(\sigma)) d\sigma \right). \quad (4)$$

Putting this into practice, we set $A(0) = 100$ units, which is equivalent to assume that A is the percent value of the initial activity.

These models have been successfully applied when studying the inactivation of various enzymes with different conditions of pressure and temperature (see [12, 21] and [22]). However, they can be used only for cases where the temperature is known (typically by experimental measurements). Therefore, these models do not allow to perform numerical optimization in general situations without temperature evolution data. Furthermore, unless we know the distribution of the temperature and its evolution inside the food, this model is only able to describe macro values for the enzymatic activity without being able to provide the possible non-homogeneous distribution of the activity inside the food. All these drawbacks will be overcome in the following sections by developing models (Section 3) that are capable of describing the distribution of temperature inside the food sample and by coupling them (Section 4) with the models presented in this section.

3 Heat and Mass Transfer Modelling

When HP is applied in Food Technology, it is necessary to take into account the thermal effects that are produced by variations of temperature due to the compression/expansion that takes place in both the food sample and the pressurizing fluid.

During and after the compression, there is heat exchange between the pressure chamber, the pressure medium and the food sample. As a result, we get a time-dependent distribution of temperatures. In the fluid medium (the pressurizing fluid and also the food sample when it is in liquid state) temperatures variation implies fluid density variation, leading to free convection during the high pressure process. Therefore, conduction and convection have been considered in these models, taking into account heat and mass transfer [3, 19].

Often, HP experiments are carried out in a cylindrical pressure vessel (typically a hollow steel cylinder) previously filled with the packed food and the pressurizing fluid. The user may choose if the food sample is going to be cooled or warmed during the process.

Due to the characteristics of this kind of processes, we assume that thermally induced flow instabilities are negligible. Therefore, axial symmetry allows us to use cylindrical coordinates and the corresponding domain given by half a cross section (intersection of the cylinder with a plane containing the axis). Let us consider four two-dimensional sub-domains (see Figure 1):

- Ω_F : domain where the food sample is located.
- Ω_C : cap of the sample holder (typically a rubber cap).
- Ω_P : domain occupied by the pressurizing medium.
- Ω_S : domain of the steel that surrounds the domains mentioned above.

Then, our domain in the (r, z) -coordinates is the rectangle $\Omega = [0, L] \times [0, H]$ defined by

$$\overline{\Omega} = \overline{\Omega_F \cup \Omega_C \cup \Omega_P \cup \Omega_S},$$

where $\{0\} \times (0, H)$ generates the axis of symmetry.

On the boundary of Ω , which is denoted by Γ , we distinguish:

- $\Gamma_r \subset \{L\} \times (0, H)$, where the temperature will be known.
- $\Gamma_{up} = [0, L] \times \{H\}$, where heat transfer with the room where the equipment is located may take place.
- $\Gamma \setminus \{\Gamma_r \cup \Gamma_{up}\}$, with zero heat flux, either by axial symmetry or by isolation of the equipment.

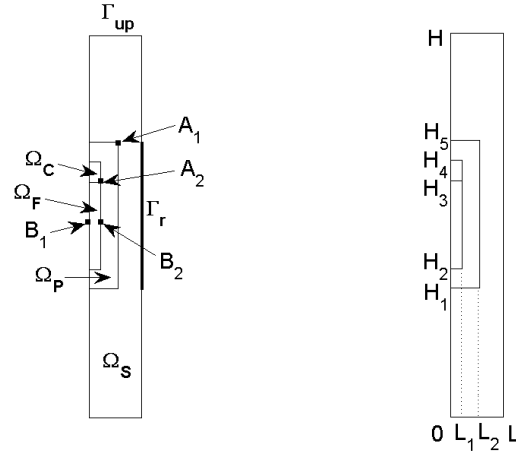


Figure 1: Computational domain.

We denote by Ω^* , Ω_F^* , Ω_C^* , Ω_P^* , Ω_S^* , Γ^* , Γ_r^* and Γ_{up}^* the domains generated when rotating Ω , Ω_F , Ω_C , Ω_P , Ω_S , $\Gamma \setminus (\{0\} \times (0, H))$, Γ_r and Γ_{up} along the axis of symmetry (in the 3D space), respectively.

For the mathematical model we distinguish two significant cases: solid and liquid type foods (see Sections 3.1 and 3.2, respectively).

3.1 Solid type foods

3.1.1 Heat transfer by conduction

When solid type foods are considered, the starting point is the heat conduction equation for the temperature T (K)

$$\rho C_p \frac{\partial T}{\partial t} - \nabla \cdot (k \nabla T) = \alpha \frac{dP}{dt} T \text{ in } \Omega^* \times (0, t_f), \quad (5)$$

where $\rho = \rho(T, P)$ is the density (Kg m^{-3}), $C_p = C_p(T, P)$ is the heat capacity ($\text{J Kg}^{-1}\text{K}$), $k = k(T, P)$ is the thermal conductivity ($\text{W m}^{-1}\text{K}^{-1}$) and t_f is the final time (s). The right hand side of the equation denotes the internal heat generation due to pressure change (see [28]). Here $P = P(t)$ is the pressure (Pa) applied by the equipment (this is chosen by the user within the machine limitations) and $\alpha = \alpha(T, P)$ is given by

$$\alpha = \begin{cases} \text{thermal expansion coefficient (K}^{-1}\text{) of the food in } \Omega_F^*, \\ \text{thermal expansion coefficient (K}^{-1}\text{) of the pressurizing fluid in } \Omega_P^*, \\ 0, \text{ elsewhere.} \end{cases}$$

This term results from the following law:

$$\frac{\Delta T}{\Delta P} = \frac{\alpha T V}{M C_p} = \frac{\alpha T}{\rho C_p},$$

where ΔT denotes the temperature change due to the pressure change ΔP , V (m^3) is the volume and M (Kg) is the mass.

The conductive heat transfer equation (5) is completed with appropriate initial and boundary conditions depending on the HP machine, in order to determine the solution that we are looking for. Here, we have used the same conditions as in [28] for a pilot unit (ACB GEC Alsthom, Nantes, France) located at the

Instituto del Frío, CSIC, Spain:

$$\left\{ \begin{array}{ll} k \frac{\partial T}{\partial \mathbf{n}} = 0 & \text{on } \Gamma^* \setminus (\Gamma_r^* \cup \Gamma_{\text{up}}^*) \times (0, t_f), \\ k \frac{\partial T}{\partial \mathbf{n}} = h(T_{\text{amb}} - T) & \text{on } \Gamma_{\text{up}}^* \times (0, t_f), \\ T = T_r & \text{on } \Gamma_r^* \times (0, t_f), \\ T(0) = T_0 & \text{in } \Omega^*, \end{array} \right. \quad (6)$$

where \mathbf{n} is the outward unit normal vector on the boundary of the domain, T_0 is the initial temperature, T_r is the refrigeration or heating temperature that stays constant in Γ_r^* (cooling or warming the food sample), T_{amb} is the (constant) ambient temperature and h ($\text{W m}^{-2}\text{K}^{-1}$) is the heat transfer coefficient.

By using cylindrical coordinates and axial symmetry, system (5)–(6) may be rewritten as the following 2D problem:

$$\left\{ \begin{array}{ll} \rho C_p \frac{\partial T}{\partial t} - \frac{1}{r} \frac{\partial}{\partial r} \left(r k \frac{\partial T}{\partial r} \right) - \frac{\partial}{\partial z} \left(k \frac{\partial T}{\partial z} \right) = \alpha \frac{dP}{dt} T & \text{in } \Omega \times (0, t_f), \\ k \frac{\partial T}{\partial \mathbf{n}} = 0 & \text{on } \Gamma \setminus (\Gamma_r \cup \Gamma_{\text{up}}) \times (0, t_f), \\ k \frac{\partial T}{\partial \mathbf{n}} = h(T_{\text{amb}} - T) & \text{on } \Gamma_{\text{up}} \times (0, t_f), \\ T = T_r & \text{on } \Gamma_r \times (0, t_f), \\ T(0) = T_0 & \text{in } \Omega. \end{array} \right. \quad (7)$$

This model is suitable when the filling ratio of the food sample inside the vessel is much higher than the one of the pressurizing medium. This has been shown in [28], where the model has been validated with several comparisons between numerical and experimental results. In [28] they also show that when the filling ratio of the food inside the vessel is not much higher than the one of the pressure medium, the solution of this model is very different from the experimental measurements. Two ways of solving that inconvenience are the following:

- (i) To use the same model but with an apparent conductivity value for the pressurizing medium higher than the real one. This method will not give good results for the temperature distributions in the pressurizing fluid but can give acceptable results inside the food. We are not going to discuss this possibility in this paper.
- (ii) As shown in [28], the model can be improved by including the convection phenomenon that takes place in the pressurizing medium. The resulting model is more expensive from a computational point of view but the results are more accurate. We discuss this methodology in Section 3.1.2.

3.1.2 Heat transfer by conduction and convection

The non-homogeneous temperature distribution induces a non-homogeneous density distribution in the pressurizing medium and consequently a buoyancy fluid motion. In other words, free convection.

This fluid motion may strongly influence the temperature distribution. In order to take into account this fact, a non-isothermal flow model is considered. Therefore, we suppose that the fluid velocity field, \mathbf{u} (m s^{-1}), satisfies the Navier–Stokes equations for compressible Newtonian fluid under Stoke’s assumption

(see, for instance, [1]). The resulting system of equations is:

$$\left\{ \begin{array}{l} \rho C_p \frac{\partial T}{\partial t} - \nabla \cdot (k \nabla T) + \rho C_p \mathbf{u} \cdot \nabla T = \alpha \frac{dP}{dt} T \quad \text{in } \Omega^* \times (0, t_f), \\ \rho \frac{\partial \mathbf{u}}{\partial t} - \nabla \cdot \eta (\nabla \mathbf{u} + \nabla \mathbf{u}^t) + \rho (\mathbf{u} \cdot \nabla) \mathbf{u} \\ \quad = -\nabla p - \frac{2}{3} \nabla (\eta \nabla \cdot \mathbf{u}) + \rho \mathbf{g} \quad \text{in } \Omega_{\mathbf{P}}^* \times (0, t_f), \\ \frac{\partial \rho}{\partial t} + \nabla \cdot (\rho \mathbf{u}) = 0 \quad \text{in } \Omega_{\mathbf{P}}^* \times (0, t_f), \end{array} \right. \quad (8)$$

where \mathbf{g} is the gravity vector (m s^{-2}), $\eta = \eta(T, P)$ is the dynamic viscosity (Pa s), $p = p(x, t)$ is the pressure generated by the mass transfer inside the fluid, and $P + p$ is the total pressure (Pa) in the pressurizing medium $\Omega_{\mathbf{P}}^*$.

We point out that on the right hand side of the first equation of (8) we could have written $\alpha \frac{d(P+p)}{dt} T$, but we have supposed that the internal heat generation due to mass transfer is negligible. On the right hand side of the second equation of (8) we have written ∇p , since $P = P(t)$ depends only on time and therefore $\nabla(P + p) = \nabla p$. As in the previous section, the density $\rho = \rho(T, P)$ is a known state function.

System (8) has been completed with appropriate point, boundary and initial conditions:

$$\left\{ \begin{array}{ll} k \frac{\partial T}{\partial \mathbf{n}} = 0 & \text{on } \Gamma^* \setminus (\Gamma_{\mathbf{r}}^* \cup \Gamma_{\text{up}}^*) \times (0, t_f), \\ k \frac{\partial T}{\partial \mathbf{n}} = h(T_{\text{amb}} - T) & \text{on } \Gamma_{\text{up}}^* \times (0, t_f), \\ T = T_{\mathbf{r}} & \text{on } \Gamma_{\mathbf{r}}^* \times (0, t_f), \\ \mathbf{u} = 0 & \text{on } \Gamma_{\mathbf{P}}^* \times (0, t_f), \\ T(0) = T_0 & \text{in } \Omega^*, \\ p = 10^5 & \text{in } \mathbf{A}_1 \times (0, t_f), \end{array} \right. \quad (9)$$

where \mathbf{A}_1 is a corner point of $\Gamma_{\mathbf{P}}^*$, which is the boundary of $\Omega_{\mathbf{P}}^*$.

We remark that the point condition at \mathbf{A}_1 means that the total pressure ($P + p$) at this point is equal to the equipment pressure P plus the atmospherical pressure.

As shown in Section 3.1.1 for the conductive heat transfer model (see system (7)), system (8)–(9) can be also rewritten as an equivalent 2D problem by using cylindrical coordinates (we do not write here the resulting system). All the numerical experiments that have been considered in this paper were carried out on the 2D version of the corresponding equations.

3.2 Liquid type foods

For liquid type foods we propose a model considering that convection also occurs in the region Ω_F and we distinguish two separated velocity fields, \mathbf{u}_F and \mathbf{u}_P , for the food and the pressurizing fluid, respectively. We point out that the pressurizing medium and the food are separated by the sample holder and do not mix. As in Section 3.1.2, we assume that the pressurizing fluid is compressible and Newtonian.

Note that in this case the convection plays again an important role, not only in the pressurizing fluid, but also in the liquid type food sample. Therefore, the neglect of its effect (as done in the solid case), would produce results that would be very different to the real thermal behaviour. A detailed dimensional analysis for equations involving convection phenomena during high pressure treatment of liquid media can be found in [19].

Assuming that the food is a compressible Newtonian fluid, the governing equations are

$$\left\{ \begin{array}{l} \rho C_p \frac{\partial T}{\partial t} - \nabla \cdot (k \nabla T) + \rho C_p \mathbf{u} \cdot \nabla T = \alpha \frac{dP}{dt} T \quad \text{in } \Omega^* \times (0, t_f), \\ \rho \frac{\partial \mathbf{u}_F}{\partial t} - \nabla \cdot \eta (\nabla \mathbf{u}_F + \nabla \mathbf{u}_F^t) + \rho (\mathbf{u}_F \cdot \nabla) \mathbf{u}_F \\ \quad = -\nabla p - \frac{2}{3} \nabla (\eta \nabla \cdot \mathbf{u}_F) + \rho \mathbf{g} \quad \text{in } \Omega_F^* \times (0, t_f), \\ \rho \frac{\partial \mathbf{u}_P}{\partial t} - \nabla \cdot \eta (\nabla \mathbf{u}_P + \nabla \mathbf{u}_P^t) + \rho (\mathbf{u}_P \cdot \nabla) \mathbf{u}_P \\ \quad = -\nabla p - \frac{2}{3} \nabla (\eta \nabla \cdot \mathbf{u}_P) + \rho \mathbf{g} \quad \text{in } \Omega_P^* \times (0, t_f), \\ \frac{\partial \rho}{\partial t} + \nabla \cdot (\rho \mathbf{u}_F) = 0 \quad \text{in } \Omega_F^* \times (0, t_f), \\ \frac{\partial \rho}{\partial t} + \nabla \cdot (\rho \mathbf{u}_P) = 0 \quad \text{in } \Omega_P^* \times (0, t_f), \end{array} \right. \quad (10)$$

with point, boundary and initial conditions:

$$\left\{ \begin{array}{l} k \frac{\partial T}{\partial \mathbf{n}} = 0 \quad \text{on } \Gamma^* \setminus (\Gamma_r^* \cup \Gamma_{up}^*) \times (0, t_f), \\ k \frac{\partial T}{\partial \mathbf{n}} = h(T_{\text{amb}} - T) \quad \text{on } \Gamma_{up}^* \times (0, t_f), \\ T = T_r \quad \text{on } \Gamma_r^* \times (0, t_f), \\ \mathbf{u}_F = 0 \quad \text{on } \Gamma_F^* \times (0, t_f), \\ \mathbf{u}_P = 0 \quad \text{on } \Gamma_P^* \times (0, t_f), \\ T = T_0 \quad \text{in } \Omega^*, \\ p = 10^5 \quad \text{in } \mathbf{A}_1 \times (0, t_f), \\ p = 10^5 \quad \text{in } \mathbf{A}_2 \times (0, t_f), \end{array} \right. \quad (11)$$

where Γ_F^* denotes the boundary of Ω_F^* and \mathbf{A}_1 , \mathbf{A}_2 are corner points of Γ_P^* and Γ_F^* , respectively (see Figure 1). As in the previous sections, we will use a 2D-axially symmetric version of (10)–(11).

We point out that when the food is a non-Newtonian fluid, the second equation of system (10) should be replaced by the corresponding momentum balance equation. This complicates considerably the model and will not be considered here.

3.3 Full models considered

For practical purposes, in the following sections we are going to focus only on two relevant situations:

- Solid type food with a big filling ratio. According to the results of [28] discussed at the end of Section 3.1.1, we will consider system (7) as the corresponding full model (denoted by SFull).
- Liquid type food with a small filling ratio. In this case, equations (10)–(11) will be considered as the full model (denoted by LFull).

3.4 Model sensitivity

In practice, the coefficients used in equations (7)–(11) are usually approximated using experimental data with a standard deviation lower than $\pm 5\%$ of the value [31]. Furthermore, due to equipment limitations, some experimental discrepancies could occur during the process (for instance, the pressure curve could be not strictly respected, measure errors in initial temperature could occur, etc). In order to study the impact of those errors on the temperature and enzymatic activity evolutions during the process, we perform a sensitivity study on the considered models.

More precisely, we generate $N \in \mathbb{N}$ perturbed models (with corresponding temperature solutions T_{per} , $\text{per} = 1, 2, \dots, N$) from the original one, with ρ , C_p , k , α , η , T_0 , T_r and P perturbed randomly by $\pm 5\%$. To perform the sensitivity analysis, for an arbitrary function $f : D \rightarrow \mathbb{R}$ with $D \subset \mathbb{R}^p$, we define the mean value

$$\mathcal{M}(f; D) = \frac{1}{|D|} \int_D f(z) dz, \quad (12)$$

where $|D|$ is the measure of D . Then, we compute the average of the mean temperature errors

$$\text{AET} = \frac{1}{N} \sum_{\text{per}=1}^N \mathcal{M}(|T - T_{\text{per}}|; \Omega \times (0, t_f)), \quad (13)$$

that will be compared with the mean temperature $\mathcal{M}(T; \Omega \times (0, t_f))$, in order to obtain the corresponding percent relative error

$$\text{RAET} = 100 \times \frac{\text{AET}}{\mathcal{M}(|T|; \Omega \times (0, t_f))}. \quad (14)$$

Since the enzymatic activity model studied in Section 2 needs as an input the temperature only of the food sample, we highlight the behaviour of the models when focusing on the domain Ω_F . To do that, we define the average temperature error in the food sample, AET_F , and the corresponding percent relative error, RAET_F , by changing Ω by Ω_F in (13) and (14), respectively.

3.5 Simplified models

In order to reduce the computational complexity needed to solve the full models (7) and (10)–(11), it is interesting to consider some simplified versions (called ‘simplified models’), that are cheaper to evaluate and with results that do not vary too much from those of the full models. Indeed, simplified models are useful when they are used, for example, during optimization processes that need to solve the models many times for different data [14, 17, 29].

We carry out the study of the numerical characteristics of one simplified version of the solid type food model (7) and two simplified versions of the liquid type food model (10)–(11) described previously.

For the solid type food we consider a simplified model with constant coefficients, by setting C_p , k , α , ρ and η to their mean value (\bar{C}_p , \bar{k} , $\bar{\alpha}$, $\bar{\rho}$ and $\bar{\eta}$, respectively) in the range of temperature and pressure considered in the process. This model is denoted by SCC.

On the other hand, for the liquid type food we consider a first simplified model with constant coefficients, as in the SCC model, except for the density ρ , which remains dependent on temperature and pressure (in order to keep the effect of the gravitational forces). This model is denoted by LCC.

The second simplified model for the liquid case is based on the Boussinesq approximation. More precisely, the coefficients C_p , k , α and η are considered to be constant as in the LCC model; ρ is also chosen as a constant value $\bar{\rho}$, except for the gravitational force $\rho \mathbf{g}$ that appears in the second and third equation of the system (10). Furthermore, the food and the pressurizing fluids are assumed to be incompressible. This model is denoted by LB and given by

$$\left\{ \begin{array}{ll} \bar{\rho} \bar{C}_p \frac{\partial T}{\partial t} - \bar{k} \nabla^2 T + \bar{\rho} \bar{C}_p \mathbf{u} \cdot \nabla T = \bar{\alpha} \frac{dP}{dt} T & \text{in } \Omega^* \times (0, t_f), \\ \bar{\rho} \frac{\partial \mathbf{u}_F}{\partial t} - \bar{\eta} \nabla^2 \mathbf{u}_F + \bar{\rho} (\mathbf{u}_F \cdot \nabla) \mathbf{u}_F = -\nabla p + \rho \mathbf{g} & \text{in } \Omega_F^* \times (0, t_f), \\ \bar{\rho} \frac{\partial \mathbf{u}_P}{\partial t} - \bar{\eta} \nabla^2 \mathbf{u}_P + \bar{\rho} (\mathbf{u}_P \cdot \nabla) \mathbf{u}_P = -\nabla p + \rho \mathbf{g} & \text{in } \Omega_P^* \times (0, t_f), \\ \nabla \cdot \mathbf{u}_F = 0 & \text{in } \Omega_F^* \times (0, t_f), \\ \nabla \cdot \mathbf{u}_P = 0 & \text{in } \Omega_P^* \times (0, t_f), \end{array} \right. \quad (15)$$

with boundary and initial conditions given by (11).

We are interested in evaluating the efficiency of the simplified models. With this aim, we compare the simplified model SCC with the full model SFull and the simplified models LCC and LB with the full model

LFull. More precisely, denoting by T_{sim} the temperatures obtained by solving each of them, we compute the mean error committed in the whole domain,

$$\text{ET} = \mathcal{M}(|T - T_{\text{sim}}|; \Omega \times (0, t_f)), \quad (16)$$

and the corresponding percent relative error

$$\text{RET} = 100 \times \frac{\text{ET}}{\mathcal{M}(|T|; \Omega \times (0, t_f))}. \quad (17)$$

As in Section 3.5, we emphasize the behaviour of the models focusing on the domain Ω_F . To do that, we define ET_F , and RET_F , by taking Ω_F instead of Ω in (16) and (17), respectively.

3.6 Numerical tests

For the numerical experiments we have considered the size of the pilot unit (ACB GEC Alsthom, Nantes, France) that was used in [28]. More precisely, $L = 0.09$ m, $H = 0.654$ m, $L_2 = 0.05$ m, $H_1 = 0.222$ and $H_5 = 0.472$ m (see Figure 1).

We work with the two representative examples described in Section 3.3. The size and location of the sample and the rubber cap are given by $H_3 = 0.404$ m and $H_4 = 0.439$ in both cases; $L_1 = 0.045$ m and $H_2 = H_1$ in the solid case, and $L_1 = 0.02$ m and $H_2 = 0.294$ m in the liquid case (see Figure 1).

We present numerical tests computed in cylindrical coordinates using the Finite Element Method (FEM) solver COMSOL Multiphysics 3.4. Velocity and pressure spatial discretization is based on P2–P1 Lagrange Finite Elements satisfying the Ladyzhenskaya, Babuska and Brezzi (LBB) stability condition. The time integration is performed using the Variable–Step–Variable–Order (VSVO) BDF–based strategy implemented in this platform. The nonlinear systems are solved with a damped Newton method. The algebraic linear systems are solved using UMFPACK (Unsymmetric MultiFrontal method for sparse linear systems) combined with the stabilization technique GLS (Galerkin Least Squares). All computations for the numerical tests have been performed on a Quad–Core processor with 3.4 GHz/Core and 8Gb of RAM.

The physical parameters of the pressurizing medium and the liquid type food are supposed to be equal to those of water and dependent on temperature and pressure. More precisely, ρ , C_p and k are computed through a *shifting approach* [27] from atmospheric pressure. For the parameter α we use the expression described in [26]. Finally, dynamic viscosity η is computed by a piecewise linear interpolation, with data obtained from [20].

On the other hand, we have chosen tylose as an example of solid type food. This gel has similar properties to meat [25]. The corresponding coefficients are obtained from [27] for atmospheric pressure. A rescaling procedure [9, 25] and a piecewise linear interpolation have been applied for other values of pressure.

For general cases, where the thermophysical properties of a particular food are unknown, mathematical tools for inverse problems may be needed to identify these parameters. For example, in [7] the authors discuss how to identify the heat transfer coefficient for a particular prototype. Identification of coefficients depending on temperature is considered in [6], in a rigorous mathematical way, for a general abstract framework.

In both cases, liquid and solid type food, the thermophysical properties of the steel and the rubber cap of the sample holder are assumed to be constant. More precisely, $\rho = 7833$ Kg m⁻³, $C_p = 465$ J Kg⁻¹K⁻¹ and $k = 55$ W m⁻¹K⁻¹ for steel and $\rho = 1110$ Kg m⁻³, $C_p = 1884$ J Kg⁻¹K⁻¹ and $k = 0.173$ W m⁻¹K⁻¹ for rubber are taken.

The ambient temperature, the reference temperature and the heat transfer coefficient used in the tests are $T_{\text{amb}} = 19.3$ °C, $T_r = 40$ °C and $h = 28$ W m⁻²K⁻¹, respectively.

For each type of food, we consider two high pressure processes with different initial temperature and pressure curve:

(ii) Process P1: The initial temperature is

$$T_0 = \begin{cases} 40 \text{ °C} & \text{in } \Omega_S, \\ 22 \text{ °C} & \text{in } \Omega \setminus \Omega_S \end{cases}$$

and the pressure is linearly increased during the first 305 seconds until it reaches 600 MPa. Thus, the pressure generated by the equipment satisfies $P(0) = 0$ and

$$\frac{dP}{dt} = \begin{cases} \frac{120}{61} 10^6 \text{ Pa s}^{-1}, & 0 < t \leq 305, \\ 0 \text{ Pa s}^{-1}, & t > 305. \end{cases}$$

- (iii) **Process P2:** The initial temperature is $T_0 = 40^\circ\text{C}$ in the whole domain Ω and the pressure is linearly increased (with the same slope as before) during the first 183 seconds until it reaches 360 MPa. Thus, the pressure generated by the equipment satisfies $P(0) = 0$ and

$$\frac{dP}{dt} = \begin{cases} \frac{120}{61} 10^6 \text{ Pa s}^{-1}, & 0 < t \leq 183, \\ 0 \text{ Pa s}^{-1}, & t > 183. \end{cases}$$

For each one of these four cases (solid/liquid, P1/P2) we compute the solution of the full model described in Section 3.3, we carry out the sensitivity analysis explained in Section 3.4 and we calculate the solutions for the simplified models described in Section 3.5.

3.6.1 Full model analysis

Figure 2 shows the temperature distribution for both solid and liquid type food, under processes P1 and P2, at time $t = 15$ min. Time-averaged temperature distribution (i.e., the function $x \mapsto \mathcal{M}(T(x, \cdot); (0, t_f))$, for $x \in \Omega$) for the four cases is represented in Figure 3. The evolution of the sample mean temperature (i.e., the function $t \mapsto \mathcal{M}(T(\cdot, t); \Omega_F)$, for $t \in [0, t_f]$) is depicted in Figure 4, which also shows the evolution of the temperature at two points (see Figure 1): the first one, \mathbf{B}_1 , is located at the center of the sample (in the symmetry axis) and the second one, \mathbf{B}_2 , on the surface of the sample, at the same height as \mathbf{B}_1 .

These figures illustrate how the model captures the non-homogeneous temperature distribution inside the domain and the different behaviour between the solid and liquid cases. For instance, in the liquid case, the temperature distribution is more homogeneous than in the solid case, due to mass transfer. Therefore, the model and the numerical approximation of its solution is consistent with what is physically expected.

As already remarked in [28] for solid type foods, our numerical experiments show that for liquid type food it can also be interesting to use an initial food temperature lower than T_r (as done in process P1), in order to anticipate the temperature increase that results from compression. This allows us to get a more uniform process, avoiding big temperature gradients inside the food as well as much higher than T_r temperatures (we remind that one of the goals of the high-pressure technology is to process the food without using high temperatures, which degrade some of the main qualities of food). Figure 4 shows this behaviour for process P1.

3.6.2 Model sensitivity analysis

According to Section 3.4, in order to evaluate the sensitivity of the models, we have generated $N = 10$ perturbed versions of the full models (with random perturbations of $\pm 5\%$). Table 1 summarizes the obtained results. The average AET of the mean temperature errors in the whole domain, defined in (13), is less than 1.15°C , which represents a relative error (see (14)) of 2.83%. Furthermore, the average AET_F of the mean temperature errors in the sample is less than 1.45°C and the relative error is less than 3.34%. We remark that both relative errors are of the order of the parameter perturbations, which shows the robustness of the models.

3.6.3 Simplified model analysis

In this section we check the efficiency of the simplified models introduced in Section 3.5 and present the results in Table 2.

We can see that the mean temperature error in the sample is bigger than in the whole domain. This is due to the fact that the thermophysical parameters for the steel and the rubber cap are the same for the

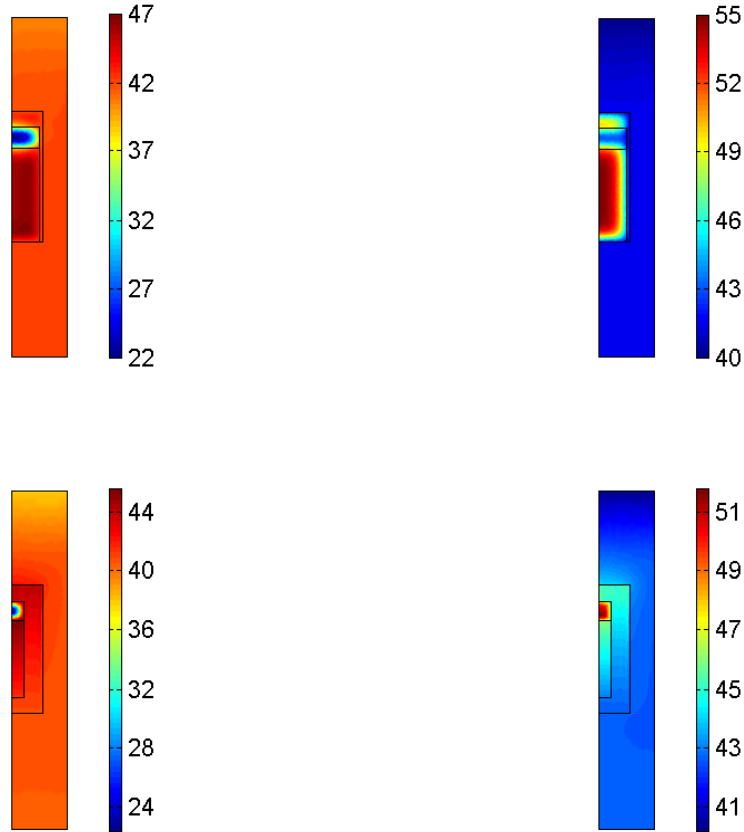


Figure 2: Temperature distribution ($^{\circ}\text{C}$) in the whole domain at $t = 15$ min for solid (**Top**) and liquid (**Bottom**) food cases after processes P1 (**Left**) and P2 (**Right**).

full and the simplified models. Therefore the differences are concentrated in the food and the pressurizing fluid. Nevertheless, the mean temperature relative errors in the food sample are quite acceptable, since the sensitivity analysis performed in Section 3.6.2 reveal an average mean relative error of the same order.

Comparing the processes, we observe that the error made in the three simplified models (SCC, LCC and LB) is less important in process P2 than in process P1. This is due to the fact that the range of pressure and temperature in P2 is smaller than in P1 and therefore, the approximation of parameters by their mean value is better in P2.

Comparing solid and liquid type foods, we observe that the errors made in the simplified models are smaller in the liquid cases than in the solid ones. The different size of the temperature ranges (larger for solid type food samples) that are obtained at each time explains this behaviour.

Comparing the computational times we observe that in the solid case we have a reduction by a factor of 13 while in the liquid case this factor is less than 2. The reason is that the SCC model becomes linear but the LCC and LB remain nonlinear. In any case, LCC and LB have similar errors, but LB is faster and easier to implement on the computer.

The reduction of computational time combined with acceptable errors reveal that the simplified models are a good alternative to the full ones for optimization procedures.

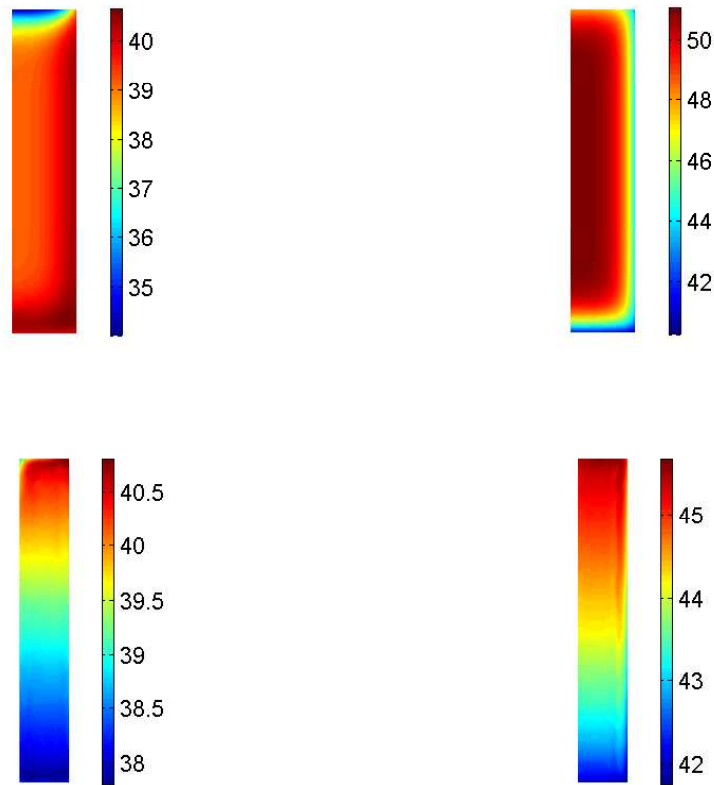


Figure 3: Time-averaged temperature distribution ($^{\circ}\text{C}$) during 15 min in the solid (**Top**) and liquid (**Bottom**) food sample after P1 (**Left**) and P2 (**Right**) processes.

4 Coupling of Enzymatic Inactivation and Heat–Mass Transfer Models

In this section we couple the heat transfer models presented in Section 3 with the kinetic equation (1). This allows us to get a model capable of describing non-homogeneous activity distribution inside the food. Moreover, we perform a numerical study of the impact of various HP–Thermal processes on the inactivation of three different enzymes: Bacillus Subtilis α –Amylase (BSAA), Lipoxygenase (LOX) and Carrot Pectin Methyl–Esterase (CPE).

4.1 Resulting activity equation

The activity distribution is expressed in a different way for solid type food (where the particles are considered to be motionless) and for liquid type food (where the particles are considered to move due to mass transfer).

4.1.1 Solid type foods

For solid type foods we have supposed that the particles do not move. Thus, according to (4), the activity A of a particle located at the point $x \in \Omega_{\text{F}}$ at time t can be written as

$$A(x, t) = A(x, 0) \exp \left(- \int_0^t \kappa(P(\sigma), T(x, \sigma)) d\sigma \right). \quad (18)$$

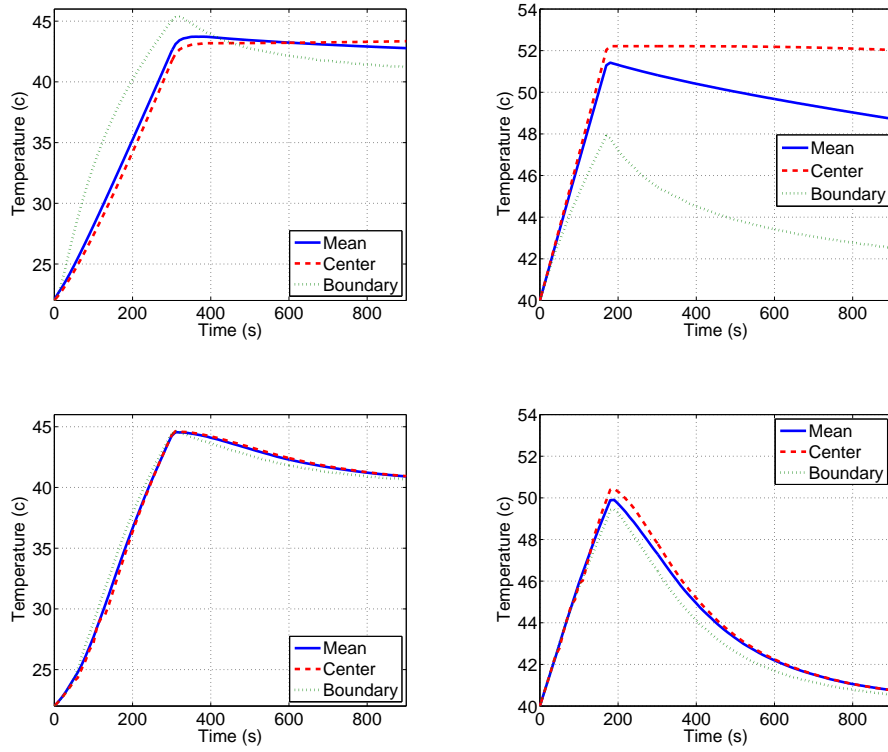


Figure 4: Evolution of the sample mean temperature (—), temperature in the center point B_1 (- -) and in the boundary point B_2 (...) (see Figure 1) during the processes P1 (Left) and P2 (Right) in the solid (Top) and liquid (Bottom) food samples.

The equipment pressure P (MPa) is a given function (we assume that the mass transfer pressure p is negligible compared to P) and the temperature T (K) is obtained by solving system (7).

4.1.2 Liquid type foods

For liquid type foods, the particles move in the food domain Ω_F due to mass transfer. In this case, for each point $x \in \Omega_F$ we consider the trajectory of a food particle that ends at point x . This trajectory X is the solution of

$$\begin{cases} \frac{dX}{dt}(t) = \mathbf{u}_F(X(t), t), & t \in (0, t_f), \\ X(t_f) = x, \end{cases} \quad (19)$$

where \mathbf{u}_F is the velocity field computed by solving system (10)–(11). Therefore, according to (4) again, the activity A of a particle located at the point $x \in \Omega_F$ at time t can be expressed as

$$A(x, t) = A(X(0), 0) \exp\left(-\int_0^t \kappa(P(\sigma), T(X(\sigma), \sigma)) d\sigma\right). \quad (20)$$

In this case, $T(X(t), t)$ is obtained by solving system (10)–(11). Here, $X(t)$ is the point that the trajectory X reaches at time t .

4.2 Discretization of the activity equation

Let us consider a time discretization given by $0 = t_0 < t_1 < \dots < t_n = t_f$ with step $\tau = t_i - t_{i-1} = \frac{t_f}{n}$ for $i = 1, 2, \dots, n$.

Process	Food	Whole domain			Sample		
		MT	AET	RAET	MT _F	AET _F	RAET _F
P1	Solid	39.39	1.08	2.74	39.37	1.32	3.34
P2	Solid	41.46	1.14	2.75	49.25	1.45	2.93
P1	Liquid	39.77	1.07	2.68	39.06	1.05	2.70
P2	Liquid	40.49	1.15	2.83	43.95	1.17	2.67

Table 1: MT: Mean temperature $\mathcal{M}(T; \Omega \times (0, t_f))$ (°C); AET: Average mean temperature error (°C) (see (13)); RAET: Relative average mean temperature error (%) (see (14)); MT_F, AET_F, RAET_F: Idem for the food sample, changing Ω by Ω_F .

Process	Model	Whole domain			Sample			CT
		MT	ET	RET	MT _F	ET _F	RET _F	
P1	SFull	39.39	—	—	39.37	—	—	53
P2	SFull	41.46	—	—	49.25	—	—	51
P1	SCC	39.71	0.30	0.77	41.38	1.88	4.77	4
P2	SCC	41.50	0.04	0.10	49.53	0.25	0.52	4
P1	LFull	39.77	—	—	39.06	—	—	3135
P2	LFull	40.49	—	—	43.95	—	—	4141
P1	LCC	39.90	0.16	0.41	39.95	0.81	2.07	2459
P2	LCC	40.48	0.03	0.06	43.94	0.09	0.20	2877
P1	LB	39.89	0.15	0.37	39.89	0.77	1.96	2196
P2	LB	40.47	0.03	0.08	43.94	0.10	0.22	2475

Table 2: Results obtained for full and simplified models. MT: Mean temperature $\mathcal{M}(T; \Omega \times (0, t_f))$ (°C); ET: Mean temperature error (°C) (see (16)); RET: Relative mean temperature error (%) (see (17)); MT_F, ET_F, RET_F: Idem in the food sample; CT: Computational time (s) needed to solve the model.

4.2.1 Solid type foods

Given $x \in \Omega_F$ and denoting $\kappa_j(x) = \kappa(P(t_j), T(x, t_j))$, a numerical approximation of (18) can be obtained considering, for instance, the trapezoidal formula

$$A(x, t_n) \approx A(x, 0) \exp \left(-\frac{\tau}{2} \sum_{j=0}^{n-1} \left(\kappa_j(x) + \kappa_{j+1}(x) \right) \right). \quad (21)$$

The enzymatic activity is evaluated on a equally distributed mesh in the food sample domain Ω_F .

4.2.2 Liquid type foods

For each point $x \in \Omega_F$ let X be the trajectory of a particle satisfying $X(t_f) = x$. We take an approximation $\{X_i\}_{i=0}^n$ of $\{X(t_i)\}_{i=0}^n$ defined by discretizing (19) with the following backward implicit scheme

$$\begin{cases} X_n = x \\ X_i = X_{i+1} - \tau \mathbf{u}_F(X_i, t_i), \quad i = n-1, n-2, \dots, 0. \end{cases} \quad (22)$$

The solution of (22) is computed by solving numerically the minimization problem

$$\min_{y \in \Omega_F} \|X_{i+1} - y - \tau \mathbf{u}_F(y, t_i)\|_2. \quad (23)$$

We use a Steepest–Descent algorithm starting from the solution of the backward explicit scheme

$$y_i^{(0)} = X_{i+1} - \tau \mathbf{u}_F(X_{i+1}, t_{i+1}),$$

that has to be iterated until reaching $y_i^{(m)} \in \Omega_F$ such that

$$\|X_{i+1} - y_i^{(m)} - \tau \mathbf{u}_F(y_i^{(m)}, t_i)\|_2 < 10^{-4} \|X_{i+1} - y_i^{(0)}\|_2.$$

By denoting $\kappa_j(X) = \kappa(P(t_j), T(X_j, t_j))$, a numerical approximation of (20) can be computed by considering

$$A(x, t_n) \approx A(X_0, 0) \exp \left(-\frac{\tau}{2} \sum_{j=0}^{n-1} (\kappa_j(X) + \kappa_{j+1}(X)) \right). \quad (24)$$

Again, the enzymatic activity is evaluated on a equally distributed mesh in the food sample domain Ω_F .

4.3 Enzymes considered for numerical simulation

For the numerical experiments, the following enzymes and corresponding inactivation rates have been considered:

Bacillus Subtilis α -Amylase (BSAA): It is an enzyme produced by a bacteria called Bacillus Subtilis. This bacteria, present in the ground, can contaminate food and in rare occasions cause intoxications. This enzyme catalyzes the hydrolysis of starch, generating sugars (as maltose) that can modify the taste of the food. The inactivation rate κ is modelled using equation (2) with $P_{\text{ref}} = 500 \text{ MPa}$, $T_{\text{ref}} = 313 \text{ K}$, $\kappa_{\text{ref}} = 9.2 \times 10^{-2} \text{ min}^{-1}$, $B = 10097 \text{ K}$ and $C = -8.7 \times 10^{-4} \text{ MPa}^{-1}$. Interested readers can find more details about the experimental protocol and the parameters determination in [21].

Lipoxygenase (LOX): This enzyme is present in various plants and vegetables such as green beans and green peas. It is responsible for the appearance of undesirable aromas in those products. Equation (3) is used to describe κ with $P_{\text{ref}} = 500 \text{ MPa}$, $T_{\text{ref}} = 298 \text{ K}$, $\kappa_{\text{ref}} = 1.34 \times 10^{-2} \text{ min}^{-1}$, $\Delta V_{\text{ref}} = -308.14 \text{ cm}^3 \text{ mol}^{-1}$, $\Delta S_{\text{ref}} = 90.63 \text{ J mol}^{-1} \text{ K}^{-1}$, $\Delta C_p = 2466.71 \text{ J mol}^{-1} \text{ K}^{-1}$, $\Delta \zeta = 2.22 \text{ cm}^3 \text{ mol}^{-1} \text{ K}^{-1}$, $\Delta \nu = -0.54 \text{ cm}^6 \text{ J}^{-1} \text{ mol}^{-1}$ (see [12] for more details).

Carrot Pectin Methyl-Esterase (CPE): Pectin Methyl-Esterase is an enzyme that is common to most vegetables. It can be present in vegetable juices producing low-methoxyl pectin. This process reduces juice viscosity and generates cloud loss (affecting juice flavor, color, texture and aroma). Here we concentrate on the Pectin Methyl-Esterase present in carrot juice (Carrot Pectin Methyl-Esterase). In this case, we apply equation (3) to model κ with $P_{\text{ref}} = 700 \text{ MPa}$, $T_{\text{ref}} = 323.15 \text{ K}$, $\kappa_{\text{ref}} = 7.05 \times 10^{-2} \text{ min}^{-1}$, $\Delta V_{\text{ref}} = -44.0124 \text{ cm}^3 \text{ mol}^{-1}$, $\Delta S_{\text{ref}} = 168.4 \text{ J mol}^{-1} \text{ K}^{-1}$, $\Delta C_p = 1376.6 \text{ J mol}^{-1} \text{ K}^{-1}$, $\Delta \zeta = -0.0339 \text{ cm}^6 \text{ J}^{-1} \text{ mol}^{-1}$, $\Delta \nu = -0.1195 \text{ cm}^6 \text{ J}^{-1} \text{ mol}^{-1}$ (see [22]).

4.4 Numerical results

For the numerical tests, we consider $t_f = 15 \text{ min}$ and $n = 900$. In the solid case, the activity is evaluated over a 10000 point equally distributed mesh in Ω_F (we point out that the models for the solid case need a very low computational time and therefore we can use a very fine mesh). On the other hand, a 25 node equally distributed mesh is chosen for the liquid type food case (much more expensive than the solid case, from a computational point of view).

We present the enzymatic activity computed for the solid and liquid type food samples under processes P1 and P2. We are also interested in studying the sensitivity of the final enzymatic activity regarding the thermophysical parameters of the models (7) and (10)–(11). Finally, we analyze this activity when considering the simplified models presented in Section 3.5, instead of the full ones.

4.4.1 Full model analysis

First of all, we focus on the enzymatic activity computed for the full models. As we can observe in Table 3 and Figure 5, the efficiency of processes P1 and P2 depends on the considered enzyme:

- For enzyme BSAA we observe that process P2 is more efficient, since the final activity is smaller. However the difference between P1 and P2 in the liquid sample case (5%) is less important than in

Process	Food	BSAA		LOX		CPE	
		MA	AEA	MA	AEA	MA	AEA
P1	Solid	49.72	4.60	33.54	6.81	87.55	2.28
P2	Solid	26.43	5.01	67.18	6.43	93.86	0.52
P1	Liquid	53.57	4.02	36.95	7.45	88.17	2.40
P2	Liquid	48.18	3.97	83.82	2.51	95.16	0.28

Table 3: Final activity for the full models and corresponding sensitivity analysis, for BSAA, LOX and CPE enzymes. MA: Mean activity in the full models at final time $t_f = 15$ min $\mathcal{M}(A(\cdot, t_f); \Omega_F)$ (%); AEA: Average mean final activity error ($^{\circ}\text{C}$) (see (25)).

the solid one (23%). This is due to the fact that the difference of the mean temperatures between P1 and P2 is bigger in the solid type food sample (10°C) than in the liquid one (5°C) (see Table 1). This is consistent with the fact that BSAA is an enzyme sensible to high temperatures [21].

- For enzyme LOX, we remark that process P1 (600 MPa) is clearly more efficient than P2 (360 MPa) in both the liquid and solid samples, due to the sensitivity of this enzyme to high pressure [12].
- For enzyme CPE, processes P1 and P2 are not as efficient as before. In any case, better results are obtained with P1. This enzyme seems to be quite resistant to both processes.

Taking into account these results, we can not privilege process P1 or P2 as a general food treatment. In fact, for each kind of enzyme, a specific optimal process could be considered.

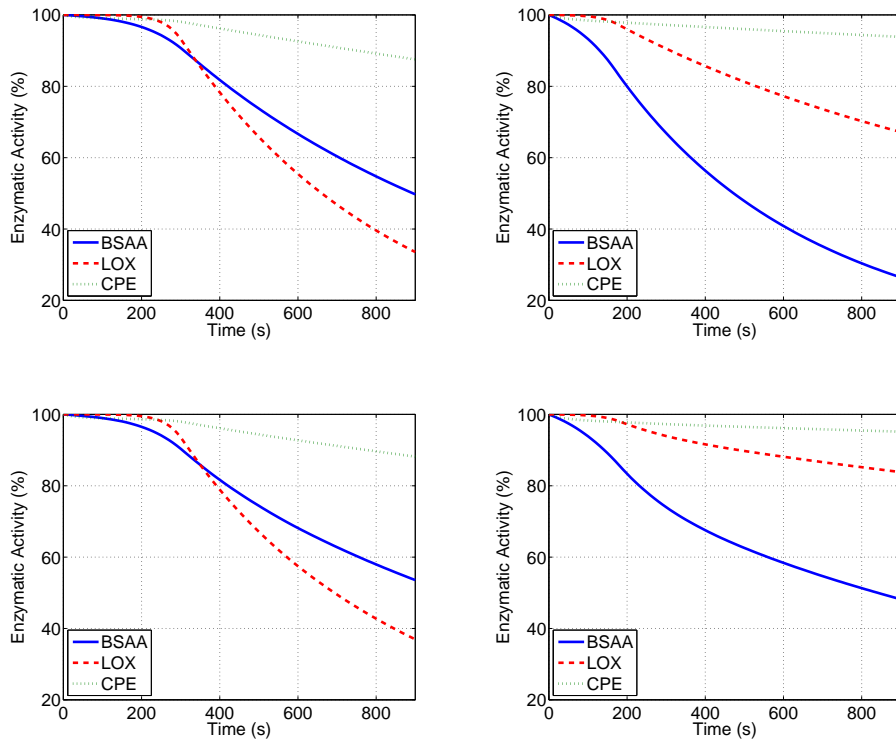


Figure 5: Enzymatic activity evolution (%) during processes P1 (Left) and P2 (Right) considering the solid (Top) and liquid (Bottom) food sample.

Figure 6 shows the final activity of enzyme LOX in the food sample for the solid and liquid cases and processes P1 and P2 (for the other enzymes, similar results are obtained). For the three considered enzymes, we can observe the following:

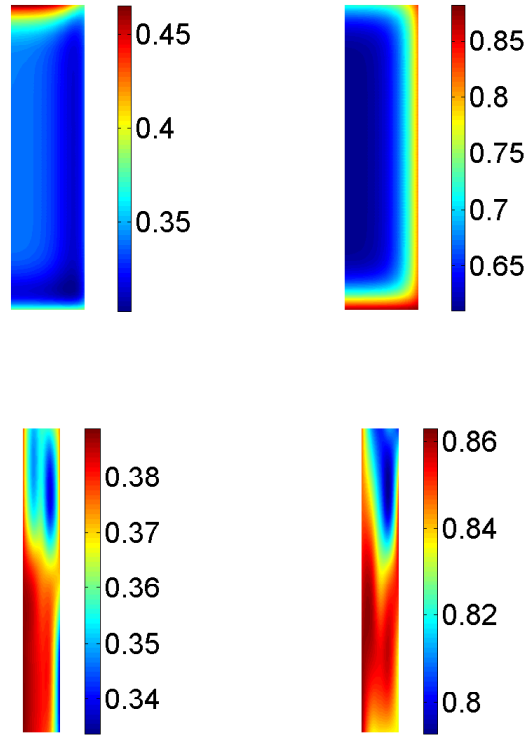


Figure 6: LOX activity distribution at $t = 15$ min in the solid (**Top**) and liquid (**Bottom**) food sample after P1 (**Left**) and P2 (**Right**) processes.

- In the solid case we obtain non-homogeneous activity distributions. Furthermore, for the considered enzymes and temperature-pressure ranges, we point out that the time-averaged temperature (see Figure 3) and final enzymatic activity distribution are related in the following way: the warmer (in time average) a zone is, the lower the final activity is. This behaviour can not be true for other enzymes and/or temperature-pressure ranges.
- In the liquid case, due to the mass transfer phenomenon, the enzymatic activity is more homogeneous than in the solid case.

4.4.2 Sensitivity analysis

We present results about final activity errors when considering the perturbed models generated in Section 3.6.2. Denoting by A_{per} the activity for the perturbed models, we define the average of the mean final activity error as

$$\text{AEA} = \frac{1}{N} \sum_{\text{per}=1}^N \mathcal{M}(|A(\cdot, t_f) - A_{\text{per}}(\cdot, t_f)|; \Omega_F). \quad (25)$$

The results obtained are reported in Table 3. We observe that perturbations of 5% of the model parameters (implying, as explained in Section 3.6.2, errors of 5% in the temperature of the food sample) generate final activity errors up to 7.45%. We deduce that the activity is relatively sensitive to pressure and temperature changes: the more sensitive to pressure and/or temperature the enzyme is, the more accurate the values of the thermophysical parameters and pressure curves should be.

4.4.3 Simplified model analysis

In this section, we study the activity A_{sim} of the simplified models introduced in Section 3.6.3. We define the mean final activity error as

$$\text{EA} = \mathcal{M}(|A(\cdot, t_f) - A_{\text{sim}}(\cdot, t_f)|; \Omega_F). \quad (26)$$

Process	Model	BSAA		LOX		CPE	
		MA	EA	MA	EA	MA	EA
P1	SFull	49.72	—	33.54	—	87.55	—
P2	SFull	26.43	—	67.18	—	93.86	—
P1	SCC	42.29	7.44	28.35	5.20	86.22	1.33
P2	SCC	25.47	0.96	66.07	1.11	93.76	0.10
P1	LFull	53.57	—	36.95	—	88.17	—
P2	LFull	48.18	—	83.82	—	95.16	—
P1	LCC	50.76	2.81	35.20	1.75	87.77	0.40
P2	LCC	47.77	1.14	83.55	0.65	95.14	0.06
P1	LB	50.56	3.04	34.97	2.00	87.72	0.45
P2	LB	47.75	2.23	83.55	1.31	95.13	0.12

Table 4: Final activity for the full and simplified models for BSAA, LOX and CPE enzymes. MA: Mean activity at final time $t_f = 15$ min $\mathcal{M}(A(\cdot, t_f); \Omega_F)$ (%); EA: Mean activity error ($^{\circ}\text{C}$) (see (26)).

As we can observe in Table 4, the errors for process P2 are smaller than for process P1. Furthermore, simplified models LCC and LB are more accurate than SCC model. This is consistent with the differences in temperature distribution obtained between those models (see Table 2). Despite these errors, simplified models are suitable when computing the enzymatic activity, since they provide an acceptable information about it with a low computational cost.

5 Concluding Remarks

The mathematical models described in this paper provide a useful tool to design and optimize processes based on the combination of thermal and high pressure processes in Food Technology. They take into account the heat and mass transfer phenomena and the enzymatic inactivation occurring during the process.

A sensitivity analysis has been developed in order to show the dependence of the solution regarding the thermophysical parameters, showing the robustness of the models.

Several simplified versions of the full models have been also proposed. When comparing them to the corresponding full model the results are quite similar. Therefore, since the simplified models need less computational time to be solved, they can be suitable for optimization procedures (which usually need to compute the solution of the corresponding model many times for different data).

All these numerical results show that there is not a general optimal treatment. For each particular kind of food and high pressure equipment we propose to carry out the following steps:

- (i) Identify the most important enzymes to be inactivated and get, for each one of them, a kinetic equation describing the evolution of their activity in terms of pressure and temperature (see Sections 2 and 4.3).
- (ii) Choose a suitable model describing the distribution of temperature in the food and solve it numerically (see Section 3).
- (iii) Use this distribution of temperature as input data for the selected kinetic equations of the enzymes, in order to get their final activities after the thermal–HP process (see Section 4).
- (iv) Perform optimization techniques (which may need to carry out several numerical experiments changing initial temperature, applied pressure, etc.) in order to reduce the enzymatic activities without using high temperatures (whose drawbacks are described in Section 3.6.1). This task may be performed with

the help of optimization software such as *Global Optimization Platform*¹ which has been validated on several benchmark [16, 18] and industrial problems [2, 13, 15].

Acknowledgment

This work was carried out with financial support from the Spanish “Ministry of Education and Science” under the projects No. MTM2007–64540, MTM2008-04621/MTM and “Ingenio Matemática (i-MATH)” No. CSD2006–00032 (Consolider–Ingenio 2010); and from the “Dirección General de Universidades e Investigación de la Consejería de Educación de la Comunidad de Madrid” and the “Universidad Complutense de Madrid” in Spain, under the project No. CCG07–UCM/ESP–2787.

The authors would also like to thank the referees for their helpful comments and suggestions.

References

- [1] R. Aris, *Vectors, Tensors, and the Basic Equations of Fluid Mechanics* (Dover Publications, Inc. New York, 1989).
- [2] L. Debiante, B. Ivorra, B. Mohammadi, F. Nicoud, A. Ern, T. Poinsot and H. Pitsch, A low-complexity global optimization algorithm for temperature and pollution control in flames with complex chemistry, *International Journal of Computational Fluid Dynamics*. **20(2)** (2006) 93–98, DOI: 10.1080/10618560600771758.
- [3] A. Delgado, C. Rauh, W. Kowalczyk and A. Baars, Review of modelling and simulation of high pressure treatment of materials of biological origin, *Trends in Food Science & Technology* **19(6)**, 329–336 (2008).
- [4] S. Denys, A. van Loey and M.E. Hendrickx, A modelling approach for evaluating process uniformity during batch high hydrostatic pressure processing: combination of a numerical heat transfer model and enzyme inactivation kinetics, *Innovative Food Science and Emerging Technologies* **1** (2000) 5–19.
- [5] K.D. Dolan, L. Yang and C.P. Trampel, Nonlinear regression technique to estimate kinetic parameters and confidence intervals in unsteady–state conduction–heated foods, *J. Food Eng.* **80** (2007) 581–593.
- [6] A. Fraguera, J.A. Infante, A.M. Ramos and J.M. Rey, Identification of a heat transfer coefficient when it is a function depending on temperature. *WSEAS Trans. Math.* **7(4)** (2008) 160–172.
- [7] B. Guignon, A.M. Ramos, J.A. Infante, J.M. Díaz and P.D. Sanz, Determining thermal parameters in the cooling of a small-scale high pressure freezing vessel. *International Journal of Refrigeration*. **29(7)** (2006) 1152–1159.
- [8] Chr. Hartman and A. Delgado, Numerical simulation of thermal and fluid-dynamical transport effects on a high pressure induced inactivation. *Simulation Modelling Practice and Theory*, vol. **13** (2005) 109–118.
- [9] Chr. Hartman, A. Delgado and J. Szymczyk, Convective and diffusive transport effect in a high pressure induced inactivation process of packed food. *Journal of Food Engineering*, vol. **59** (2003) 33–44.
- [10] R. Hayashi, Application of High Pressure to Food Processing and Preservation: Philosophy and Development. In *Engineering and Food*, vol. **2** (Elsevier Applied Science, 1989, 815–826).
- [11] I. Indrawati, A.M. van Loey, C. Smout and M.E. Hendrickx. High hydrostatic pressure technology in food preservation. In *Food preservation techniques*, P. Zeuthen and L. Bogh-Sorensen Eds. (Woodhead Publ. Ltd., Cambridge, 2003, 428–448).

¹See <http://www.mat.ucm.es/momat/software.htm>

- [12] I. Indrawati, L.R. Ludikhuyze, A.M. van Loey and M.E. Hendrickx, Lipoxygenase Inactivation in Green Beans (*Phaseolus vulgaris* L.) Due to High Pressure Treatment at Subzero and Elevated Temperatures, *J. Agric. Food Chem.* **48** (2000) 1850–1859.
- [13] D. Isebe, F. Bouchette, P. Azerad, B. Ivorra and B. Mohammadi, Optimal shape design of coastal structures, *International Journal of Numerical Method in Engineering*, Accepted, in Early view, to be published, DOI: 10.1002/nme.2209.
- [14] B. Ivorra, B. Mohammadi, L. Dumas, O. Durand and P. Redont, Semi-deterministic vs. genetic algorithms for global optimization of multichannel optical filters. *International Journal of Computational Science for Engineering.* **2(3)** (2006) 170–178, DOI: 10.1504/IJCSE.2006.012769.
- [15] B. Ivorra, B. Mohammadi and A.M. Ramos, Optimization strategies in credit portfolio management, *Journal Of Global Optimization*, Accepted, in Early view, to be published, DOI: 10.1007/s10898-007-9221-6.
- [16] B. Ivorra, B. Mohammadi, A.M. Ramos and I. Redont, Optimizing Initial Guesses to Improve Global Minimization. *Journal of Global Optimization*, submitted.
- [17] B. Ivorra, B. Mohammadi, D.E. Santiago and J.G. Hertzog, Semi-deterministic and genetic algorithms for global optimization of microfluidic protein folding devices, *International Journal of Numerical Method in Engineering*, **66(2)** (2006) 319–333, DOI: 10.1002/nme.1562.
- [18] B. Ivorra, A.M. Ramos and B. Mohammadi, Semideterministic global optimization method: Application to a control problem of the burgers equation, *Journal of Optimization Theory and Applications.* **135(3)** (2007) 549–561, DOI: 10.1007/s10957-007-9251-8.
- [19] W. Kowalczyk and A. Delgado, On convection phenomena during high pressure treatment of liquid media, *High Pressure Research* **27(1)**, 85–92 (2007).
- [20] E.W. Lemmon, M.O. McLinden and D.G. Friend, Thermophysical properties of fluid systems. In Linstrom P.J. & Mallard W.G. (Eds.), *NIST Chemistry Web Book. NIST Standard Reference Database.* **69** (June 2005). National Institute of Standards and Technology. Gaithersburg MD, 20899 (<http://webbook.nist.gov>).
- [21] L. R. Ludikhuyze, I. van den Broeck, C. A. Weemaes and M. E. Hendrickx, Kinetic Parameters for Pressure–Temperature Inactivation of *Bacillus subtilis* α -Amylase under Dynamic Conditions, *Biotechnol. Prog.*, American Chemical Society and American Institute of Chemical Engineers, **13** (1997) 617–623.
- [22] B. Ly–Nguyen, A.M. van Loey, C. Smout, S.E. Özcan, D. Fachin, I. Verlent, S. Vu Truong, T. Duvetter and M.E. Hendrickx, Mild–Heat and High–Pressure Inactivation of Carrot Pectin Methylsterase: A Kinetic Study, *Journal of Food Science*, Institute of Food Technologists. **68(4)** (2003) 1377–1383.
- [23] A. Melinder. *Thermophysical properties of liquid secondary refrigerants* (International Institute of Refrigeration, 1997).
- [24] K. Miyagawa and K. Suzuki, Studies on Taka–amylase A under high pressure: Some kinetic aspects of pressure inactivation of Taka–amylase, *A. Arch. Biochem. Biophys.* **105** (1964) 297–302.
- [25] T. Norton and D.W. Sun, Recent Advances in the Use of High Pressure as an Effective Processing Technique in the Food Industry. *Food Bioprocess Technol* **1** (2008) 2–34, doi:10.1007/s11947-007-0007-0
- [26] L. Otero, A.D. Molina–García and P.D. Sanz, Some interrelated thermophysical properties of liquid water and ice I. A user–friendly modeling review for food high–pressure processing, *Critical Reviews in Food Science and Nutrition*, **42(4)** (2002) 339–352.

- [27] L. Otero, A. Ousegui, B. Guignon, A. Le Bail and P.D. Sanz, Evaluation of the thermophysical properties of tylose gel under pressure in the phase change domain. *Food Hydrocolloids*, **20** (2006) 449—460, doi:10.1016/j.foodhyd.2005.04.001.
- [28] L. Otero, Á.M. Ramos, C. de Elvira and P.D. Sanz, A Model to Design High-Pressure Processes Towards an Uniform Temperature Distribution, *J. Food Eng.* **78** (2007) 1463–1470, doi:10.1016/j.jfoodeng.2006.01.020.
- [29] A.M. Ramos, R. Glowinski and J. Periaux, Pointwise control of the Burgers equation and related Nash equilibrium problems: computational approach. *Journal of Optimization Theory and Applications*. **112(3)** (2002) 499–516.
- [30] K. Suzuki and K. Kitamura, Inactivation of enzyme under high pressure: Studies on the kinetics of inactivation of α -amylase of *Bacillus subtilis* under high pressure., *J. Biochem.* **54(3)** (1963) 214–219.
- [31] A. Tansakul and P. Chaisawang, Thermophysical properties of coconut milk. *Journal of Food Engineering*, **73(3)** (2006) 273–280, DOI:10.1016/j.jfoodeng.2005.01.035.